IEEE Transactions on Nuclear Science, Vol.NS-24, No.3, June 1977

MICROWAVE DEVELOPMENTS AT SLAC*

Z. D. Farkas, H. A. Hogg, G. A. Loew and A. R. Wilmunder
Stanford Linear Accelerator Center, Stanford University, Stanford, California 94305

Summary

Three microwave development projects presently undertaken by the Accelerator Physics Department at SLAC are reviewed. The first is SLED (SLAC Energy Development). Some theoretical work is mentioned, and a few details of installation and control are given. The latest beam-test results are presented. Microwave beam-position monitors are the second project to be discussed. Details of two very sensitive systems which have been developed and tested are given. Finally, the use of a fast digital phase-shifter to compensate for beam-loading transients is described.

SLED (SLAC Energy Development)

Theory of Operation

For a description of the principles of SLED, the reader is referred to earlier papers.[1,2] In parallel with the ongoing fabrication and installation program, computer analyses of the energy-gain waveforms with and without beam-loading have been made. For instance, the flat-top region experimentally observed on the energy gain curve (Fig. 1)

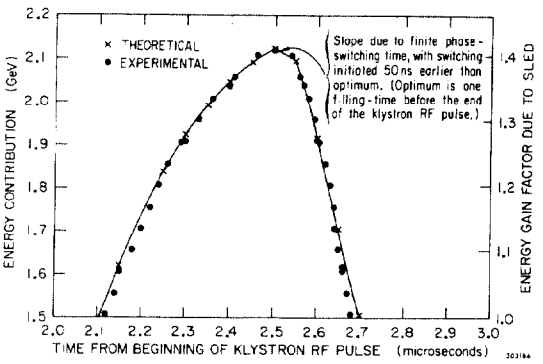

Fig. 1. Theoretical and experimental energy profiles for two SLEDded sectors.

has been shown to be due to finite phase-switching time, initiated earlier than one accelerator filling-time before the end of the klystron RF pulse. Figure 2 illustrates how beam-loading can be used to obtain good energy spectra with SLED.

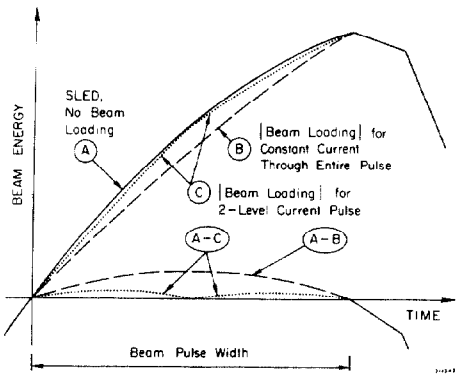

Fig. 2. Illustrating the use of beam-loading to obtain good energy spectra with SLED.

The beam pulse is always timed to end at the peak of the SLED no-load energy curve, and the beam current is adjusted so that transient beam-loading depresses the beam energy at the end of the pulse to be equal to the energy at the beginning of the beam pulse. Since the laws governing SLED energy-rise and beam-loading are different, the energy varies through the pulse as shown in curve A-B. It follows that use of a higher current in the first half of the beam pulse and a lower current in the second half can result in better matching and a smaller energy spread (curve A-C). Energy spectra have been computed for various beam pulse-widths and different combinations of SLEDded and normal sectors. For instance, if half the machine is SLEDded and half is running normally, the spectrum width for a 200 ns beam is 0.52% (constant current) and 0.14% (two currents). With the whole accelerator (30 sectors) SLEDded, the widths are 0.93% and 0.25% respectively.

Installation and Control

Prototype SLED assemblies were first thoroughly tested on the accelerator over the anticipated range of operating conditions. As a result, a number of design changes were made. Most significantly, it was found that the existing waveguide vacuum-valve (which is needed to permit klystron-replacement while the accelerator is running) could not handle the very high SLED peak RF power. It was therefore necessary to redesign the system so that the valve was fitted between the klystron and the SLED assembly. Mechanical constraints made it necessary to offset the SLED assembly at 26° with respect to the 3 km-axis and to combine the klystron adapter, monitor-coupler and pump-out into one unit. Another very significant design step was to build the SLED supporting framework out of stainless-steel tubing, and to use these tubes as distribution manifolds for the structure cooling-water. This design has resulted in a very frequency-stable structure.

Ninety-four SLED assemblies have been built so far. Sixty-three of them have been installed in Sectors 15 through 22 in the klystron gallery.

The SLED cavities can be detuned (for normal accelerator operation) by inserting tungsten needles, as described earlier.[1,2] The needles move about 7 inches from tuned to detuned positions. The outer end of each needle is attached to an armature which slides (on ceramic rods) inside a stainless-steel tube. The armature is magnetically coupled to an external permanent magnet, which in turn is driven by an electric linear-actuator. At the limits of travel, micro-switches detect the reactive force between armature and magnet, and hence give a true "tuned/detuned" status signal, which is relayed from a station control panel to a sector summary panel and thence to the Main Control Center (MCC). The actuators, which are controlled from MCC, take seven seconds to move between limits. The klystron modulator triggers are removed during this interval.

The 180° drive phase-shift which is necessary for SLED operation is applied by a PIN-diode phase-shift keying (PSK) unit in the sub-booster drive to each sector. The PSK trigger can also be controlled from MCC.

Beam-Test Results

Five-sector SLED tests were run during November 1976, with excellent results. Each sector was SLEDded individually, and its energy profile as a function of time (c.f., Fig. 1) was measured with a 30 ns probing beam. All five sectors were then SLEDded simultaneously and a combined energy increase of 1.55 GeV (corresponding to a gain of 1.41 over the non-SLEDded energy) was measured.

Microwave Beam-Position Monitors

Complete descriptions of the beam position monitors (BPM's) installed when SLAC was built, and the BPM's described briefly here, are available.[3,4,5]

BPM's with Homodyne Receiver Systems

Polarized electron-beam experiments at SLAC have required very precise beam-position monitoring to direct the beam onto the target. Two monitors were built, each capable of detecting less than 10 μm displacements of a 100 μA peak beam.

*Supported by the Energy Research and Development Admin.

These monitors used the TM_{120} rectangular resonant position cavities already present in the SLAC switchyard. A cavity of this type is shown schematically in Fig. 3. The

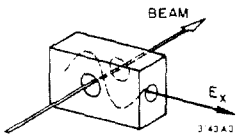

Fig. 3. Schematic of TM_{120} position cavity.

beam-induced signal amplitude E_x from this cavity varies approximately linearly with horizontal displacement x from the central axis, if the displacement is small. That is, $E_x = k_x Ix$, where I is the beam current and k_x is a constant. The phase of E_x changes by π when the beam crosses the central axis. Thus a phase-measurement will give the sense of the displacement. The cavities are grouped in orthogonal pairs to give both horizontal and vertical readouts. There is also a TM_{010} reference cavity in each set, but the latter was not used in the system being described. The X- and Y-cavities are each connected to a homodyne receiver channel, shown schematically in Fig. 4. The signal from the

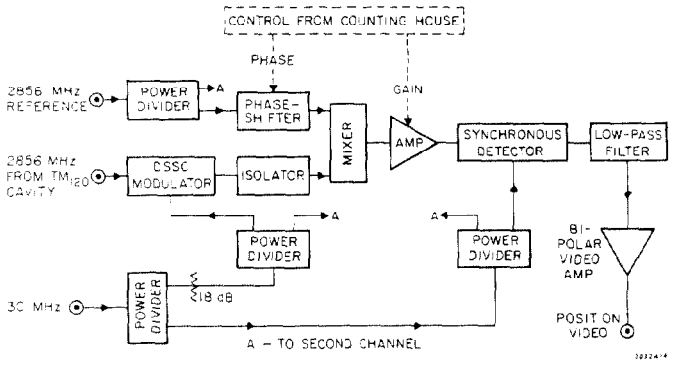

Fig. 4. Block diagram of homodyne receiver system.

position cavity, which will be on the order of -73 dBm for a 100 μA beam displaced 10 μm from the center line, is fed into a hybrid which is used as a double sideband suppressed carrier (DSSC) modulator. The modulation is produced by a relatively high-level (10 dBm) 30 MHz CW signal. The 30 MHz modulated 2856 MHz cavity signal passes through an isolator to a mixer which is used as a phase-detector. Here it is mixed with a coherent 2856 MHz CW reference signal derived from the accelerator drive system. The output of the mixer is a 30 MHz signal.

The phase of the reference signal into the mixer can be remotely adjusted to maximize the output amplitude, which occurs when the input signal vectors are colinear. The mixer output is amplified and fed into a synchronous detector, where it is phase-compared with part of the original 30 MHz signal. Again, it is necessary to adjust the phase of one 30 MHz signal to maximize the video output from the synchronous detector. A low-pass filter removes the residual 30 MHz signal, and the video passes through a bipolar video amplifier to ADC circuits and an SDS 9300 computer available to the experimenter.

The system described may be set up to give positive video polarity when the beam is, say to the right of center. It is important to note that when the beam is centered, the cavity output and its dependent signals throughout the receiver chain go to zero. No balancing is involved. When the beam moves to the left of center, the cavity output changes phase by 180°, and is followed by the DSSC and mixer output phases. This causes the video output of the synchronous detector to change polarity.

One monitor was installed near the end of the switchyard A-line, and the other was placed near the target in End Station A. The computer was used to analyze the position data supplied by the monitors and to apply corrective steering currents to vernier coils on the beam line magnets. Because of their absolute accuracy, toroids were used to monitor the beam current and thus provide the normalizing information required to compute displacement. The two position monitors were found to be sensitive to a few microns displacement.

Traveling-Wave Beam-Position Monitors (TWBPM's)

A second type of microwave BPM has been developed, in which the transducer is simply a length of S-band waveguide with beam apertures centrally placed in the broad walls. Each end of the waveguide is terminated by a matched transition to coaxial line, and the two lines are connected to a phase bridge, represented by a simple hybrid. Using the notation of Fig. 5, the hybrid output signals will be

$$E_{1,2}^2 = E^2(1 \pm \cos\theta) \qquad (1)$$

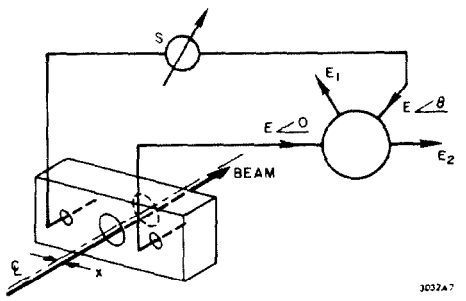

Fig. 5. Schematic of traveling-wave beam position monitor.

The phase-shifter S is adjusted so that when the beam is centered, $\theta = \pi/2$ and $E_1^2 - E_2^2 = 0$. When the beam moves off center a distance x, the additional phase-shift, ϕ, developed across the hybrid is $4\pi x/\lambda_g$, where λ_g is the effective guide wavelength. Then

$$E_{1,2}^2 = E^2(1 \pm \sin\phi) \qquad (2)$$

For small ϕ, $E_{1,2} \sim E(1 \pm \phi/2)$, and

$$E_1 - E_2 = E\phi = kIx \qquad (3)$$

where k is a constant.

A very convenient way of removing the I-dependence is shown in Fig. 6. The $E\angle 0$ and $E\angle\theta$ signals from the transducer are down-converted to 60 MHz and passed through limiter amplifiers before phase detection.

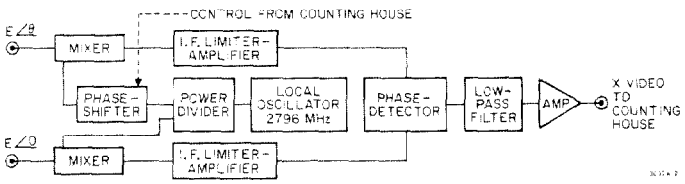

Fig. 6. Block diagram of TWBPM detection system.

Referring again to Fig. 6, the 60 MHz limiter amplifiers used have an input signal range from -70 dBm to +10 dBm. The levelled output is about +3 dBm and the transmission phase-shift over the input signal range is less than 10 degrees. However, the amplifiers in the matched pair used were specified to track to within 3 degrees. Shielding and isolation are important to minimize crosstalk. Separate local oscillators are used for the x and y channels. The transducer beam interaction impedance is about 250 ohms, and the differential phase-shift (ϕ) is 2 degrees per mm of beam displacement. The video output of each phase detector

is amplified and transmitted to the Counting House (Experimental Control Room), where it is digitized and used to monitor instantaneous beam-coordinates so that steering corrections can be computed and applied.

The monitor described will detect beam position changes of 0.1 mm for beam currents down to 20 μA.

Transient Beam-Loading Compensation

Beam loading effects on the SLAC accelerator have been previously described.[6] First-order compensation for transient beam-loading is routinely obtained by delaying the RF pulse in one or more sectors. The rising fields in the delayed sectors can be made to approximately balance the energy depression due to beam-loading in the whole accelerator. However, the balance is imperfect because the two transient phenomena follow different laws. Obviously the problem is very closely related to the technique for SLED spectrum improvement by beam-loading, described earlier in this paper.

In normal operation, the transient unbalance leads to a "gulch" in the energy spectrum. Some success in compensating for the gulch by using short RF pulses in two consecutive klystrons has been reported previously.[7] However, the method has not been used very frequently, because it is tedious to set up and maintain.

The advent of fast PIN-diode digital phase-shifters has made it possible to realize a much more direct and flexible method of transient loading compensation. A block diagram of the phase-modulating system is given in Fig. 7. The standard SLAC 1.6 μs beam-pulse time is conveniently divided into eight time-segments, each 0.2 μs long. During every pulse on a selected beam-line, the digital phase-shifter (DPS) is driven through a pattern of eight phase-shift levels (one level for each 0.2 μs time segment). During the inter-pulse period, the eight-word data set defining one phase-shift pattern is fed at a 10 kHz rate into serial in/out shift-registers. The stored words are then clocked out at a 5 MHz rate to the DPS during the beam pulse. The holding registers are necessary to avoid commutation problems. The desired data-set values are adjusted by the operator.

As a first experiment, the DPS was inserted into the sub-booster RF drive in Sector 28. A 10 GeV, 9.6 mA beam was set up and analyzed through 0.5% slits. The transmitted beam current exhibited the gulch shown in Fig. 8(a). The phase of Sector 28 (with six klystrons being used on the experimental beam) had been rotated about 30 degrees off optimum, to allow energy modulation through phase modulation. By adjusting the data-set values in the first five time-segments, the gulch was easily removed, as shown in Fig. 8(b). The experiment was repeated successfully a number of times, using different beam setup conditions. A permanent installation, controlled from MCC, is planned for the near future.

Acknowledgments

The authors gratefully acknowledge that the current success of the projects described in the paper is due in large measure to the excellent design, development and testing work done by H. Deruyter, J. Hodgers and J. M. Zamzow (on SLED), and by H. L. Martin (on the Beam Position Monitors and Transient Beam-Loading Compensation).

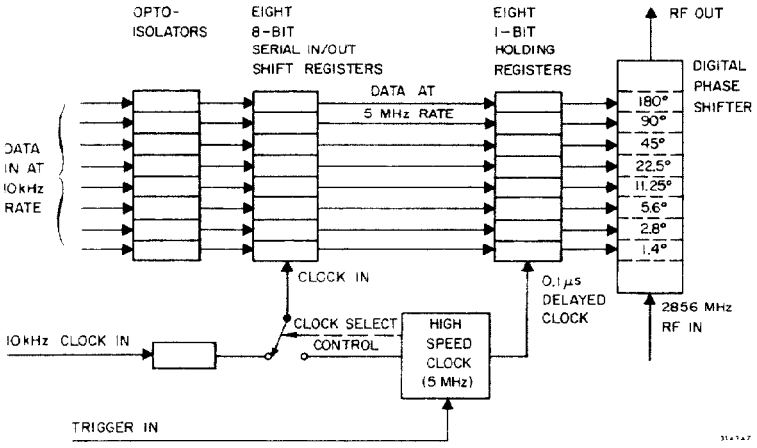

Fig. 7. Block diagram of digital phase-shifter and driver.

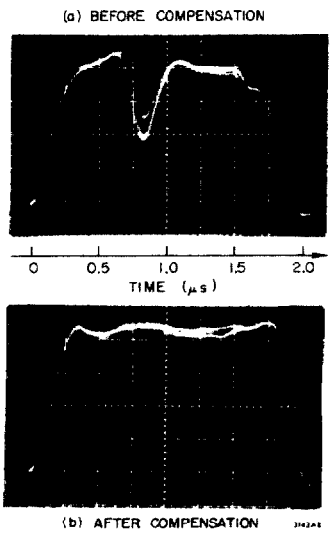

Fig. 8. Energy gulch filling on a 10-GeV beam, using a fast digital phase-shifter.

References

1. Z. D. Farkas, H. A. Hogg, G. A. Loew, P. B. Wilson, "SLED: A Method of Doubling SLAC's Energy," Proc. IXth Int. Conf. on High Energy Accelerators, SLAC, Stanford, California, May 2-7, 1974, p. 576.
2. Z. D. Farkas, H. A. Hogg, G. A. Loew, P. B. Wilson, "Recent Progress on SLED, The SLAC Energy Doubler," IEEE Trans. Nuc. Sci. NS-22, No. 3, 1299 (June 1975).
3. E. V. Farinholt, Z. D. Farkas, H. A. Hogg, "Microwave Beam Position Monitors at SLAC," IEEE Trans. Nuc. Sci. NS-14, 1127-1131 (June 1967).
4. R. B. Neal, ed., The Stanford Two-Mile Accelerator (W. A. Benjamin, New York, 1968), Chapter 15.
5. Z. D. Farkas, H. A. Hogg, H. L. Martin, A. R. Wilmunder, "Recent Developments in Microwave Beam-Position Monitors at SLAC," Proc. 1976 Proton Linear Accelerator Conf., CRNL, Chalk River, Ontario, Canada, September 14-17, 1976, p. 300.
6. R. B. Neal, op. cit., Chapters 6 and 14.
7. R. H. Helm, H. A. Hogg, R. F. Koontz, G. A. Loew, R. H. Miller, R. B. Neal, "Recent Beam Performance and Developments at SLAC," IEEE Trans. Nuc. Sci., NS-16, No. 3, 311 (June 1969).